Doxorubicin-Loaded Thermo- and pH-Tunable Carriers for Targeted Drug Delivery to Liver Cancer Cells *in Vitro*

The thermo- and pH-dependent DOX carriers based on MGNS, functionalized with a PNIPAM and PEI nanogel that targets liver cancer cells, were formulated and showed a high potential for microenvironment stimulus-prompted drug delivery and suppression of cancer cells.

Smart drug-delivery biomaterials that are triggered with specific stimuli, including temperature, pH and enzymatic activity, have recently been formulated. The stimulus-responsive properties of these biomaterials can offer an improved delivery of drugs to the targeted tumor sites when applied in anticancer drug delivery.[1,2] Stimulus-dependent biomaterials are promising candidates for precise control of drug delivery to targeted sites. These materials undergo rapid tunable structural changes prompted by exterior stimuli in the surrounding environment, offering a well-controlled drug release. Among stimulus-dependent biomaterials, thermo-responsive biomaterials offer exciting prospects for the controlled release of anticancer drugs, precisely to the cancer cells, whereas decreasing adverse effects on other organs.[3,4] The interior applied temperature can hence prompt the release of drugs from such biomaterials, thereby controlling the release pattern or required dosage of drugs in the targeted location. Attention should be paid to thermo-responsive nanogels, which transit because of temperature changes on adjusting their physiochemical and colloidal properties, and exhibit a phase-transition temperature, namely the lower critical solution temperature (LCST). In an aqueous solution, thermo-responsive polymers undergo rapid and changeable structural transitions from a swollen to a collapsed state, which leads to an on–off detachment of drug molecules due to temperature.[5] Moreover, pH-dependent biomaterials have been developed to release drugs in acidic tumor environments. Polymeric micelles have been incorporated with pH-sensitive components that transit to a hydrophilic state under acidic pH, causing the micelles to disassemble and to trigger the release of drugs. These pH-responsive biomaterials undergo a transition once delivered to acidic sites or in acidic tumor microenvironments.

The analyses of X-ray absorption near edge structure (XANES) and extended X-ray absorption fine structure (EXAFS) spectra were performed to understand the fine structure and the Fe atomic arrangement in terms of bond distance and co-ordination number. The XANES and EXAFS experiments were implemented at wiggler beamline **TLS 17C1**. Small-angle neutron scattering (SANS) experiments were undertaken on **BILBY** scattering equipment (OPAL research reactor) at Australian Nuclear Science and Technology Organisation (ANSTO, Australia). The structural changes of the samples were measured at temperatures 25, 37 and 42 °C.

Kuen-Song Lin (Yuan Ze University) and his group thoroughly examined the nature of the iron products using the XANES technique to obtain information related to the electronic configuration, stereochemistry and oxidation states of Fe atoms in the samples.[2,6] The XANES results

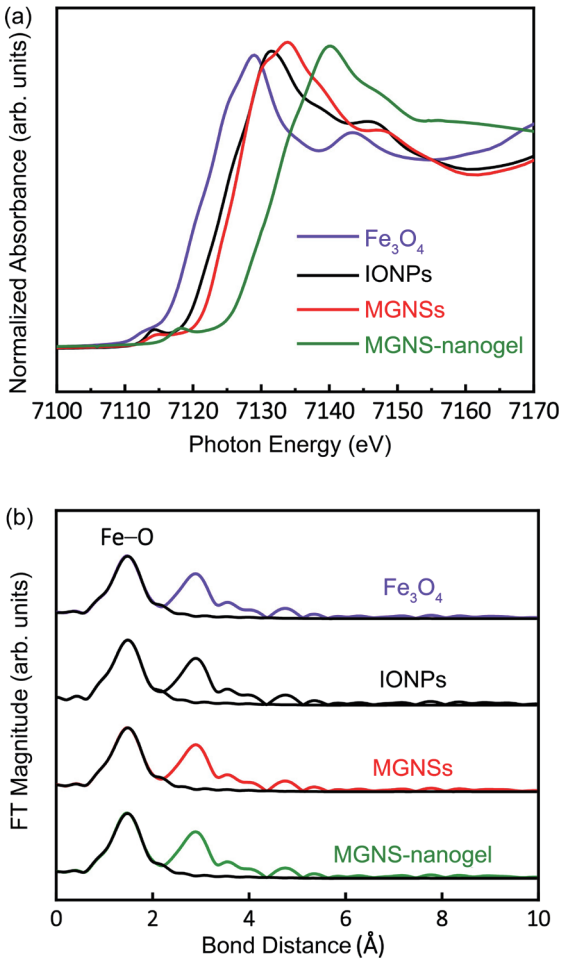

Fig. 1: (a) Fe K-edge derivative XANES spectra of Fe_3O_4, IONP, MGNS and MGNS-nanogel. (b) Fe K-edge EXAFS Fourier-transformed spectra of Fe_3O_4, IONP, MGNS and MGNS-nanogel. [Reproduced from Ref. 6]

of the Fe atom in the Fe_3O_4 standard, IONP, MGNS and MGNS-nanogel carriers displayed an absorbance signal (Fe = 7112 eV) characteristic of the 1*s* to 3*d* transition (**Fig. 1(a)**). Comparison showed that the XANES results of the carriers were similar to that of the Fe standard spectrum. For Fe, the intensity of the 1*s* to 3*d* signal of the XANES Fe K-edge was administered by the average coordination number; the oxygen (O) bonds were synchronized to the central Fe cation. The EXAFS fits for the first shell are displayed in **Table 1** and **Fig. 1(b)**, which reveal that the Fe standard, MGNS and MGNS-nanogel have Fe atoms at the center that are coordinated mainly by Fe–O. The standard Fe–O bond distances in Fe_3O_4 standard, IONP, MGNS, and MGNS-nanogel carriers were 1.96, 1.95, 1.93 and 1.92 Å with coordination numbers 3.71, 3.75, 3.74 and 3.73, respectively.[6]

Table 1: Fine-structural parameters of the samples investigated with EXAFS.

Samples	First Shell	CN (±0.05)[a]	R (±0.02Å)[b]	$\Delta\sigma^2$ (Å^2)[c]
Fe_3O_4	Fe–O	3.71	1.96	0.0019
IONPs	Fe–O	3.75	1.95	0.0046
MGNSs	Fe–O	3.74	1.93	0.0045
MGNS-nanogel	Fe–O	3.73	1.92	0.0045

[a] coordination number; [b] bond distance; [c] Debye-Waller factor.

The SANS techniques were applied to confirm the temperature sensitivity of the prepared carriers at temperatures 25, 37 and 42 °C, as displayed in **Figs. 2(a) and 2(b)**. The transition behavior of the MGNS and MGNS-nanogel carriers upon applying heat was examined. As seen in **Fig. 2(a)**, there was no difference in the scattering intensity of MGNS carriers at the different temperatures, but, as a function of temperature, an increase in the scattering intensity of the MGNS-nanogel carriers was observed (**Fig. 2(b)**).[6] When the temperature was increased from 25 to 37 °C, an increased order of the MGNS-nanogel carriers was noticed, but, between the temperatures 37–42 °C, there was a slight increase in the order mainly because the nanogel attained its maximum temperature (above LCST = 42 °C). Moreover, such a transition might result from the collapsed structure of the prepared nanogel.[6] (Reported by Kuen-Song Lin, Yuan Ze University)

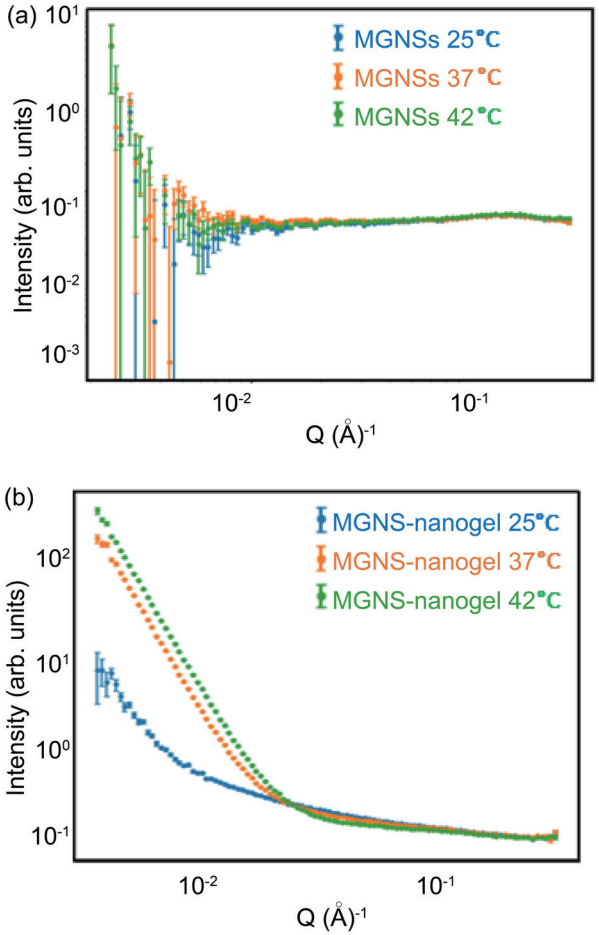

Fig. 2: SANS studies of (a) MGNS and (b) MGNS-nanogel carriers at temperatures 25, 37 and 42 °C. [Reproduced from Ref. 6]

This report features the work of Kuen-Song Lin and his collaborators published in the J. Ind. Eng. Chem. ***104****, 93 (2021).*

TLS 17C1 EXAFS
ANSTO BILBY – Small Angle Neutron Scattering

- SANS, XANES/EXAFS
- Materials Science, Chemistry, Surface, Interface and Thin-film Chemistry, Condensed-matter Physics

References

1. R. K. Dani, C. Schumann, O. Taratula, O. Taratula, AAPS PharmSciTech. **15**, 963 (2014).
2. K. Dehvari, K. S. Lin, S. S. S. Wang, Int. J. Nanosci. Nanotechnol. **14**, 361 (2014).
3. R. Cheng, F. Meng, C. Deng, H. A. Klok, Z. Zhong, Biomaterials **34**, 3647 (2013).
4. Y. Zhang, S. Uthaman, W. Song, K. H. Eom, S. H. Jeon, K. M. Huh, A. Babu, I. K. Park, I. Kim, ACS Biomater. Sci. Eng. **6**, 5012 (2020).
5. X. Lang, W. R. Lenart, J. E. Sun, B. Hammouda, M. J. Hore, Macromolecules **50**, 2145 (2017).
6. S. C. Kunene, K.-S. Lin, M.-T. Weng, M. J. C. Espinoza, C.-M. Wu, J. Ind. Eng. Chem. **104**, 93 (2021).